Devices for Space-Time Resonance Based on ECE Theory

Horst Eckardt*
Alpha Institute for Advanced Studies (A.I.A.S.)
www.aias.us

Abstract

Recently an engineering model of Einstein Cartan Evans (ECE) theory was developed. This allows the design of electro-magnetic devices under inclusion of resonance effects from space-time. The resonance is enabled by means of the spin connection which is not present in the standard model of electrical engineering (Maxwell-Heaviside theory). In this paper designs on base of the so-called vector spin connection are presented and three mathematical models are developed. The models are studied by analytical and numerical methods. Results show that space-time resonances can be evoked by these device in various ways in order to extract electrical energy from space-time. Some realization examples are proposed.

Keywords: Einstein Cartan Evans (ECE) field theory; spin connection resonance; ECE field equations; simulation model.
PACS Number:

1 Introduction

After a long period of stagnancy, general relativity has lived up by the Einstein-Cartan-Evans (ECE) theory developed by Myron Evans [1]- [4]. Space-time is considered to be the origin not only of gravity but of all forces of nature, in particular electromagnetism. Besides the curvature introduced by Einstein, torsion of Cartan geometry plays an equally weighted role in ECE theory. All electromagnetic fields are considered to be components of the torsion tensor of Cartan geometry. From this geometry two field equations are obtained which are formally identical to the well-known Maxwell-Heaviside equations in the limit of flat space-time. Therefore the ECE equations are a natural extension of the electromagnetic theory known for over 150 years.

There are three levels of mathematical representation of the ECE field equations. The most elegant and abstract level is in differential form notation. This can be evaluated to tensor form, comparable to the formalism Einstein used for his famous equation. This representation can further be rewritten to three-dimensional vector form. In this form the coordinate-independent formulation is lost, but the equations are quickly understandable to the broad majority of scientists and engineers who are not familiar with tensor calculus. The original

*e-mail: horsteck@aol.com

Cartan geometry leaves freedom of defining an extra coordinate system which describes three spatial and one timely polarisation direction (the so-called tangent space). Therefore the vectors of the E and B field have an additional index for this coordinate basis denoted by "a":

$$\begin{aligned} \mathbf{E}^a &= \left(E_x^a, E_y^a, E_z^a\right), \\ \mathbf{B}^a &= \left(B_x^a, B_y^a, B_z^a\right), \\ a &= 0 \ldots 3. \end{aligned} \tag{1}$$

This complication can be avoided by using an ordinary cartesian (or spherical/cylindrical) coordinate system as a basis for the polarisation directions in such a way that the basis vectors of polarization are identical to the unit vectors of space-time itself. Then a=1 can be identified with the x component, and a=2,3 with the y and z component respectively. The 0 component (representing the time coordinate in ECE theory) is reserved for the charge density. With this simplification we arrive at the ordinary vector definition

$$\begin{aligned} \mathbf{E} &= \left(E_x, E_y, E_z\right), \\ \mathbf{B} &= \left(B_x, B_y, B_z\right), \end{aligned} \tag{2}$$

and the ECE field equations are formally identical to Maxwell-Heaviside theory:

$$\boldsymbol{\nabla} \cdot \mathbf{B} = 0, \tag{3}$$

$$\boldsymbol{\nabla} \times \mathbf{E} + \frac{\partial \mathbf{B}}{\partial t} = 0, \tag{4}$$

$$\boldsymbol{\nabla} \cdot \mathbf{E} = \frac{\rho}{\epsilon_0}, \tag{5}$$

$$\boldsymbol{\nabla} \times \mathbf{B} - \frac{1}{c^2} \frac{\partial \mathbf{E}}{\partial t} = \mu_0 \mathbf{J}. \tag{6}$$

The difference between standard and ECE theory is made up by the potentials. The dependence of the fields E and B from the vector potential A and scalar potential ϕ is given by

$$\mathbf{E} = -\frac{\partial \mathbf{A}}{\partial t} - \boldsymbol{\nabla}\phi - c\omega^0 \mathbf{A} + \phi \boldsymbol{\omega}, \tag{7}$$

$$\mathbf{B} = \boldsymbol{\nabla} \times \mathbf{A} - \boldsymbol{\omega} \times \mathbf{A} \tag{8}$$

where $\boldsymbol{\omega}$ is the vector spin connection and ω^0 the scalar spin connection. These come into play due to the space-time torsion and curvature of Cartan geometry. Without this, the above equations would be identical to those of Maxwell-Heaviside. The spin connections forbid an arbitrary re-gauging of the potential, therefore potentials have a physical meaning in ECE theory.

2 The resonant Coulomb law

Solutions of the field equations (3-6) can be obtained by inserting the terms for the potentials (7-8) into them. This gives a set of eight non-linear equations for eight unknowns. As first stated in chapter 8 of vol. III of the ECE book series [1], some of these equations have the form of a resonance equation which is a differential equation for a function $\varphi(x)$ of the form

$$\frac{\partial^2\varphi}{\partial x^2} + 2\beta\frac{\partial\varphi}{\partial x} + \kappa_0^2\varphi = f(x) \tag{9}$$

as discussed in [10] for example (a popular explanation has also been given in [5]). In Eq. (9) β is the damping term, $f(x)$ is the driving force, and κ_0 is the eigen frequency of the system which is identical to the resonance frequency for vanishing damping [10]:

$$\kappa_R = \sqrt{\kappa_0^2 - 2\beta^2}. \tag{10}$$

From Eqs. (5) and (7) we obtain for the pure electrical case (A=0):

$$-\Delta\phi + \boldsymbol{\nabla}\cdot(\boldsymbol{\omega}\phi) = \frac{\rho}{\epsilon_0} \tag{11}$$

or

$$\Delta\phi - \boldsymbol{\omega}\cdot(\boldsymbol{\nabla}\phi) - (\boldsymbol{\nabla}\cdot\boldsymbol{\omega})\phi = -\frac{\rho}{\epsilon_0}. \tag{12}$$

This is an equation for the potential ϕ and the vector spin connection. From Eq. (12) we see that the resonance frequency has to be identified with the divergence of the spin connection:

$$\kappa_0^2 = -\boldsymbol{\nabla}\cdot\boldsymbol{\omega}. \tag{13}$$

Therefore a non-constant $\boldsymbol{\omega}$ is needed to obtain any resonance effects. In the appendix of [7] it was shown that both variables $\boldsymbol{\omega}$ and ϕ can be obtained from solving the above equation simultaneously with the Faraday equation (4). Here we simplify the situation by requesting an experimental setup which creates a vector spin connection of the desired form. According to ECE theory, the vector spin connection is to be interpreted as a rotation vector of a magnetic field. Such a situation can be realized in several ways, for example by a rotating bar magnet, a solenoid or a multi-phase AC voltage.

The situation is complicated by the fact that we need a spin connection varying in space. We can realize this in two ways: varying $\boldsymbol{\omega}$ in time and utilizing the wave propagation of $\boldsymbol{\omega}$ for an oscillation in space, or creating a gradient in one direction by a variation of the magnetic field. Experimental setups will be discussed later.

2.1 Model 1: Oscillatory model

In the following we restrict consideration to one space dimension z. Beginning with an oscillatory spin connection, we make the approach

$$\omega_z = \omega_1\cos(\kappa_1 z) \tag{14}$$

with an amplitude ω_1 and a wave number κ_1. Then Eq. (12) reads

$$\frac{\partial^2\phi}{\partial z^2} - \omega_1 \cos(\kappa_1 z)\frac{\partial\phi}{\partial z} + \omega_1\kappa_1 \sin(\kappa_1 z)\phi = f(z) \tag{15}$$

with $f(z)$ being the right-hand side of (12). Comparing this equation with Eqs. (9) and (10), the resonance frequency is

$$\kappa_R = \sqrt{\omega_1\kappa_1 \sin(\kappa_1 z) - \frac{1}{2}\omega_1^2 \cos^2(\kappa_1 z)} \tag{16}$$

which is defined only for a positive expression under the square root. Therefore the condition for the existence of resonances is

$$\omega_1\kappa_1 \sin(\kappa_1 z) - \frac{1}{2}\omega_1^2 \cos^2(\kappa_1 z) > 0 \tag{17}$$

or

$$\kappa_1 \tan(\kappa_1 z) > \frac{1}{2}\omega_1 \cos(\kappa_1 z). \tag{18}$$

This equation can be fulfilled for certain ranges of z, depending on ω_1 and κ_1. Some examples are graphed in Fig. 1. The analytical solution of Eq. (15) found by computer algebra is

$$\begin{aligned}\phi(z) = &- f(z)\, e^{\frac{\omega_1 \sin(\kappa_1 z)}{\kappa_1}} \int\int e^{-\frac{\omega_1 \sin(\kappa_1 z)}{\kappa_1}} dz dz \\ &+ f(z)\, z\, e^{\frac{\omega_1 \sin(\kappa_1 z)}{\kappa_1}} \int e^{-\frac{\omega_1 \sin(\kappa_1 z)}{\kappa_1}} dz \\ &+ k_1\, e^{\frac{\omega_1 \sin(\kappa_1 z)}{\kappa_1}} \int e^{-\frac{\omega_1 \sin(\kappa_1 z)}{\kappa_1}} dz \\ &+ k_2\, e^{\frac{\omega_1 \sin(\kappa_1 z)}{\kappa_1}}\end{aligned} \tag{19}$$

with constants k_1 and k_2. The second term represents an unbound function in z. The integrals cannot be solved analytically, therefore we present a numerical solution in Fig. 2. We used an oscillating driving force

$$f(z) = \rho_0 \cos(\kappa z). \tag{20}$$

For the parameter values $\kappa_1 = 1$, $\omega_1 = 1$ a resonant enhancement of ϕ is found for $\kappa = 1$, oscillating with a larger wavelength. These oscillations can also be seen for the non-resonant κ values, but with much shorter wave lenths. The oscillation effect of the driving force can be eliminated by setting it to a constant: $f = 1$. Fig. 3 shows the solution for such a constant driving force. This is an undamped oscillation, probably the behaviour most searched for.

The maximum amplitude differences of ϕ after 30 periods are graphed in Fig. 4. The oscillating driving force was used again. There is a resonance maximum for a driving frequency κ of about 0.1 units. Further maxima appear at integral values of κ which probably are related to the chosen value of $\kappa_1 = 1$.

2.2 Model 2: Distance model

Next we consider a spin connection decreasing by 1/z:

$$\omega_z = a_1/z \tag{21}$$

with a dimensionless factor a_1. This corresponds to a space region in vicinity of a suitable magnetic field construction (see next section). A similar model has been used for atomic structure calculations [6], [7]. Since the potential of a point charge drops by 1/z, we assume the same behaviour here for the spin connection. Then Eq. (12) becomes

$$\frac{\partial^2\phi}{\partial z^2} - \frac{a_1}{z}\frac{\partial\phi}{\partial z} + \frac{a_1}{z^2}\phi = f(z). \tag{22}$$

For $z \to 0$ the equation contains singular values but the analytical solution

$$\phi(z) = k_1\, z^{\frac{\sqrt{a_1^2-2\,a_1+1}}{2}+\frac{a_1+1}{2}} + k_2\, z^{\frac{a_1+1}{2}-\frac{\sqrt{a_1^2-2\,a_1+1}}{2}} - \frac{f(z)\,z^2}{a_1-2} \tag{23}$$

shows that there is no infinite asymptote for $z = 0$ in all cases. The last term shows that there is a resonance for $a_1 \to 2$. If $f(z)$ does not decrease faster than 1/z, the solution is growing over all bounds for $z \to \infty$. The solution contains oscillatory parts from the first two terms for $a_1 < 1$.

In Fig. 5 the regular development of the solution for z=0 can be seen ($a_1 = 1$). In the case $a_1 = -1$ (Fig. 6) there is indeed a pole if z approaches zero. In both figures we used $f = 1$.

2.3 Model 3: Linear model

A third model assumes a linear varying spin connection. A technical realization will be proposed in section 3. Assume

$$\omega_z = \gamma_1 z \tag{24}$$

with a factor $\gamma_1 > 0$ which has the units of inverse squared meters. Then Eq. (12) reads

$$\frac{\partial^2\phi}{\partial z^2} - \gamma_1 z\frac{\partial\phi}{\partial z} - \gamma_1\phi = f(z). \tag{25}$$

The analytical solution is

$$\phi(z) = -k_1\,\frac{\sqrt{2\pi}\,e^{-\frac{\gamma_1}{2}z^2}\,erf\left(\sqrt{\frac{-\gamma_1}{2}}\,z\right)}{2\,\sqrt{-\gamma_1}} + k_2\,e^{-\frac{\gamma_1}{2}z^2} + \frac{f(z)}{\gamma_1} \tag{26}$$

The behaviour of this function can be best studied from the graphs (Figs. 7 and 8). For $\gamma_1 > 0$ the solution is complex. The real part is a gaussian function with a maximum at z=0. The height of the maximum depends on the initial conditions (chosen for the left border inall cases). In all graphic examples we used

$$\phi(z_{min}) = 0,\ \frac{\partial\phi}{\partial z}(z_{min}) = 0.1\,. \tag{27}$$

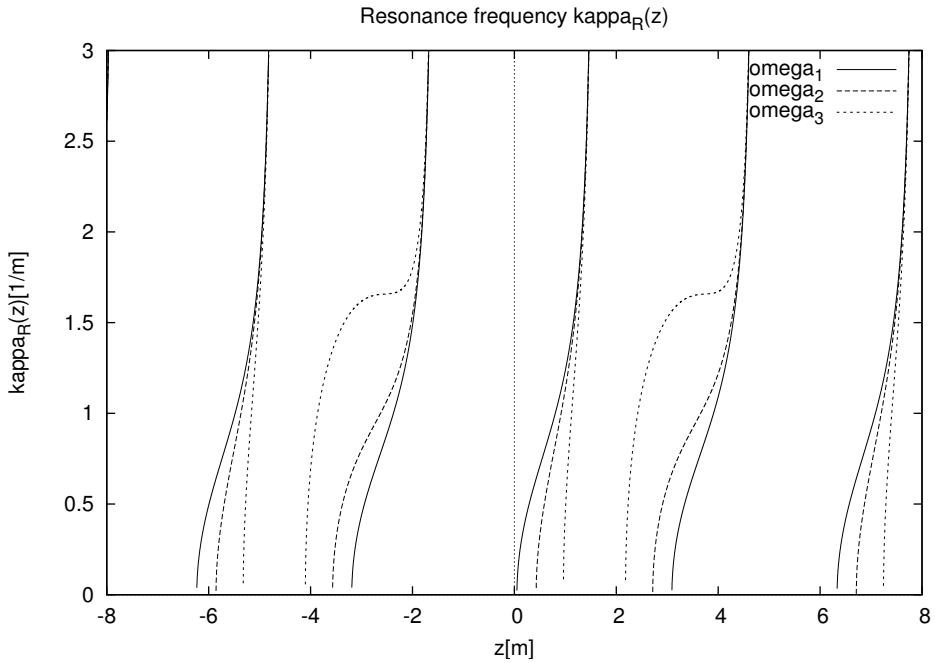

Figure 1: Range of resonance frequencies (model 1) for $\omega_1 = 0.1$, $\omega_2 = 1$, and $\omega_3 = 5$ with $\kappa_1 = 1$.

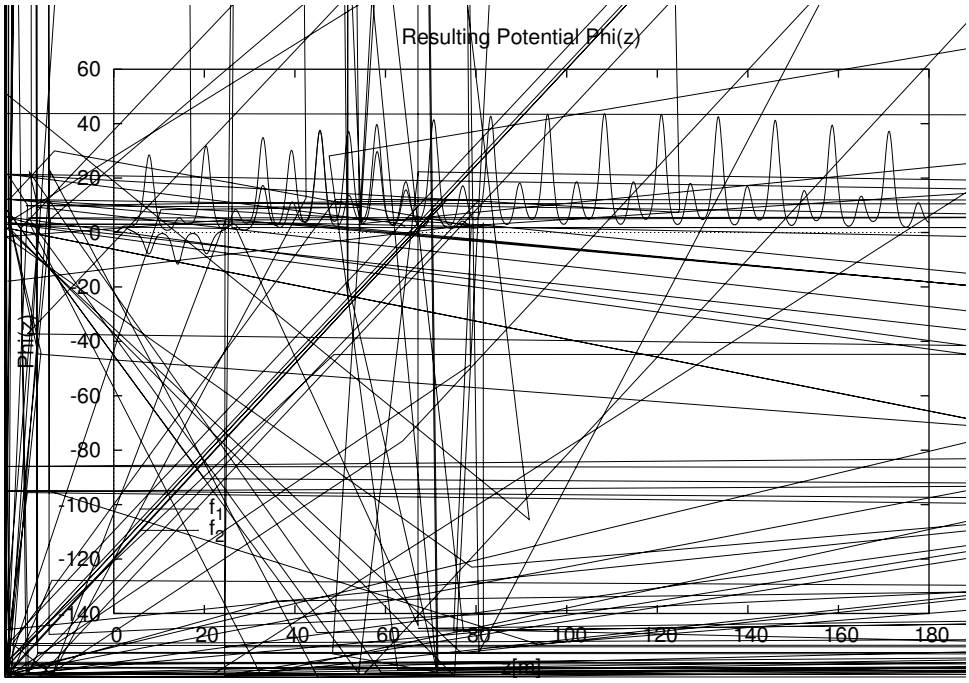

Figure 2: z dependence of Potential (model 1) for several frequencies $\kappa = 0.5, 0.9, 1.0, 1.1, 1.2$.

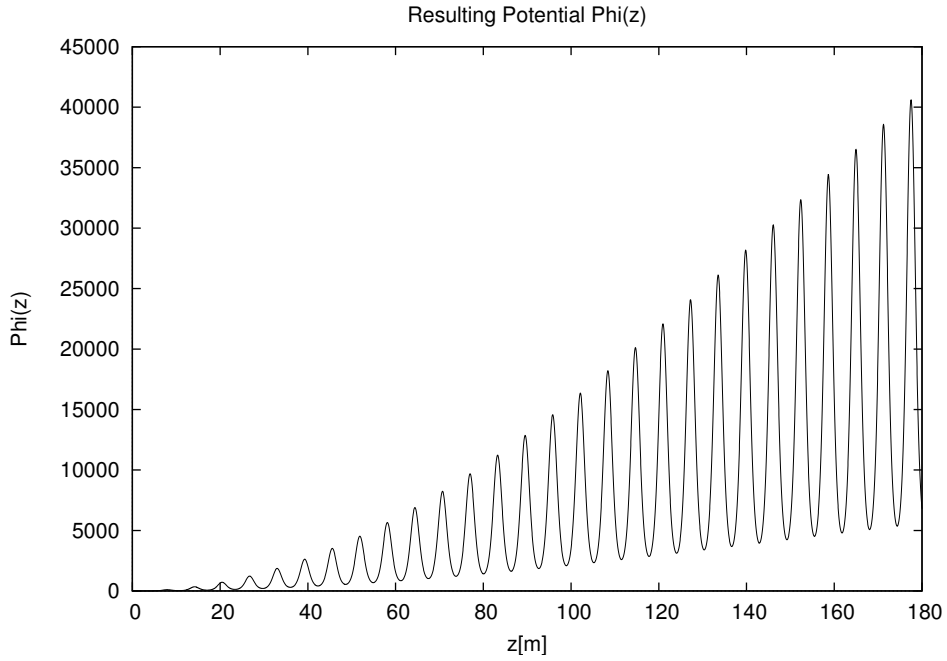

Figure 3: z dependence of Potential (model 1) for non-oscillating driving force (f=1).

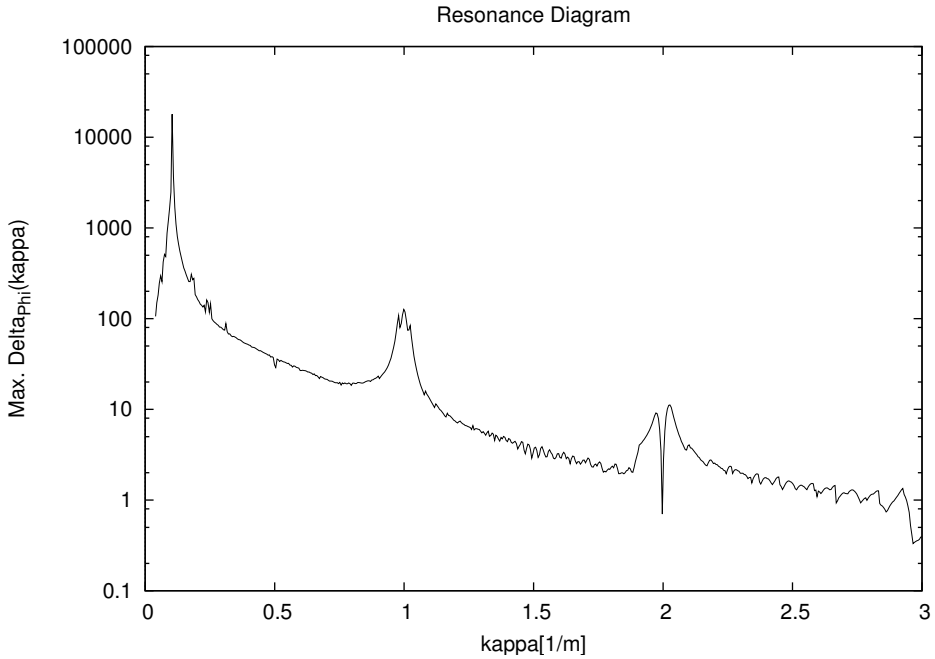

Figure 4: Resonance diagram (maximum amplitude differences) of model 1.

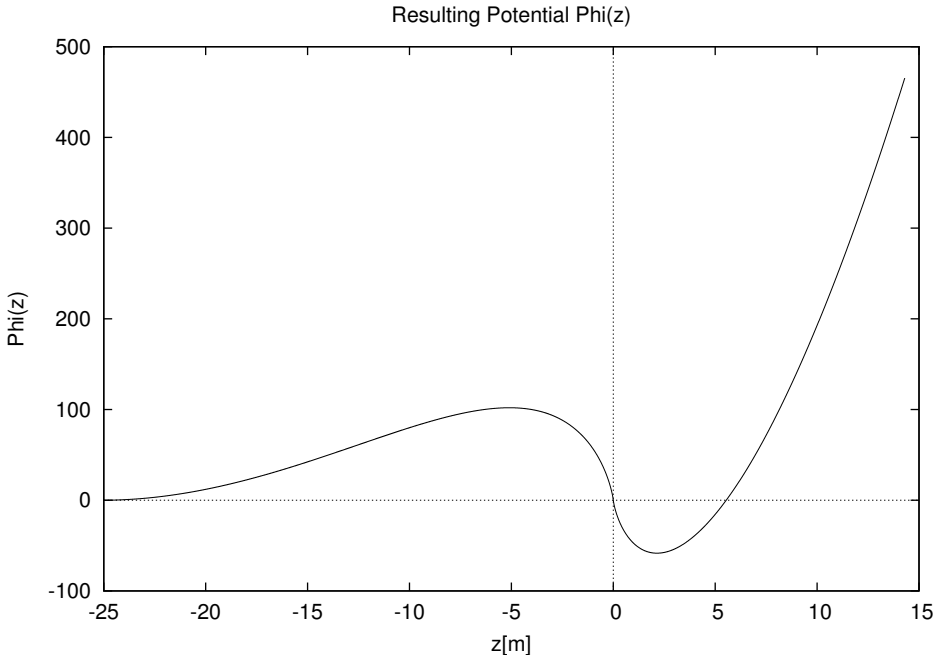

Figure 5: Solution of model 2 for $a_1 = 1$.

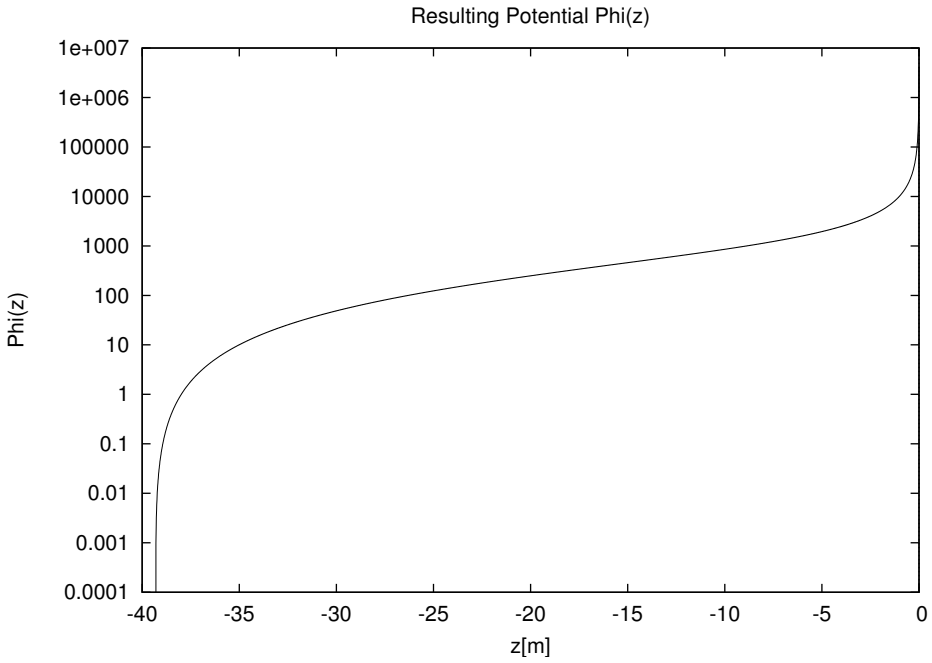

Figure 6: Solution of model 2 for $a_1 = -1$, logarithmic scale.

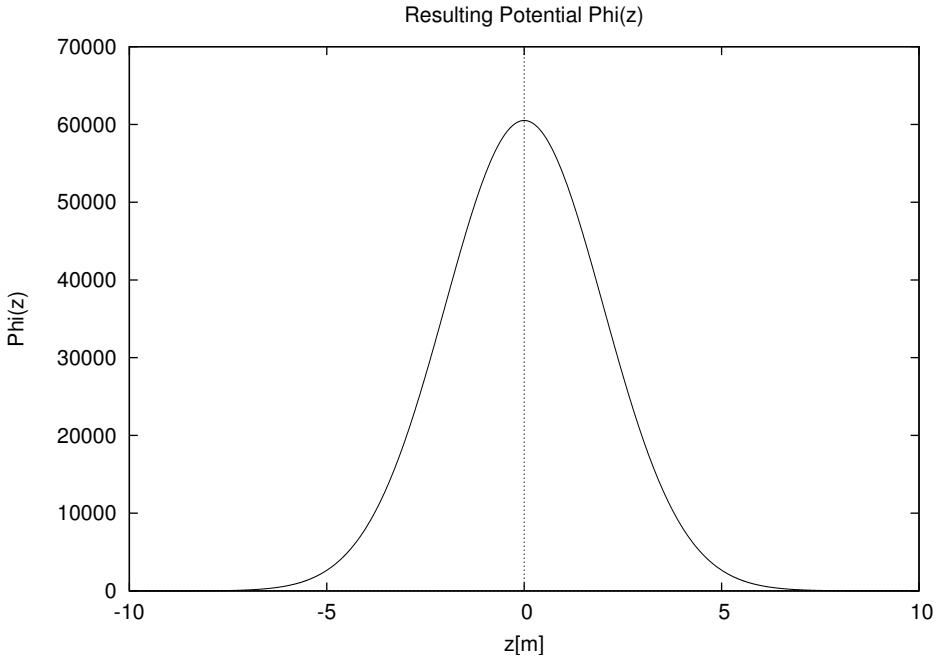

Figure 7: Solution of model 3 for $\gamma_1 = 0.25$.

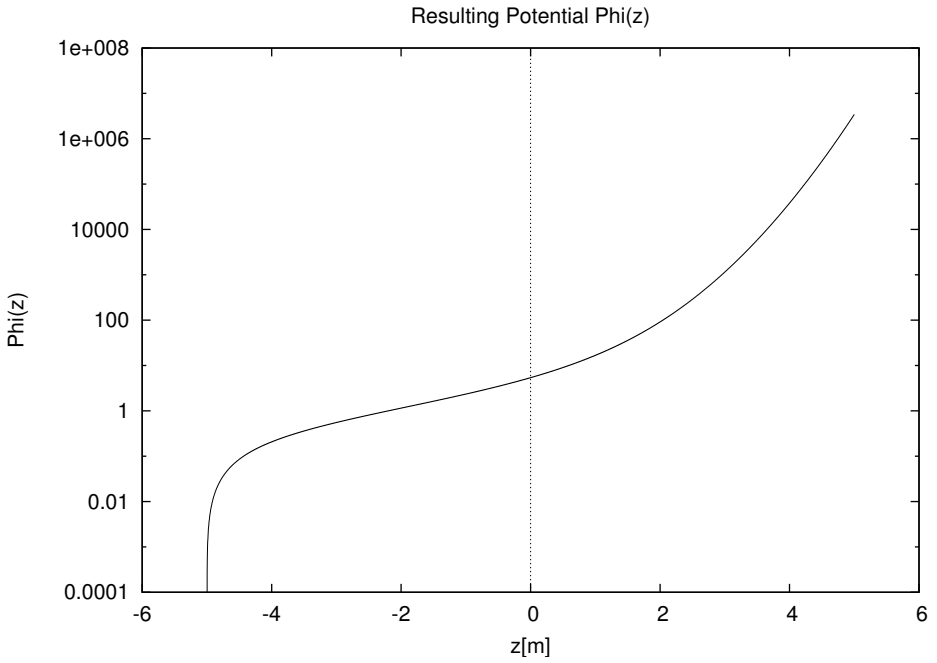

Figure 8: Solution of model 3 for $\gamma_1 = -1.0$, logarithmic scale.

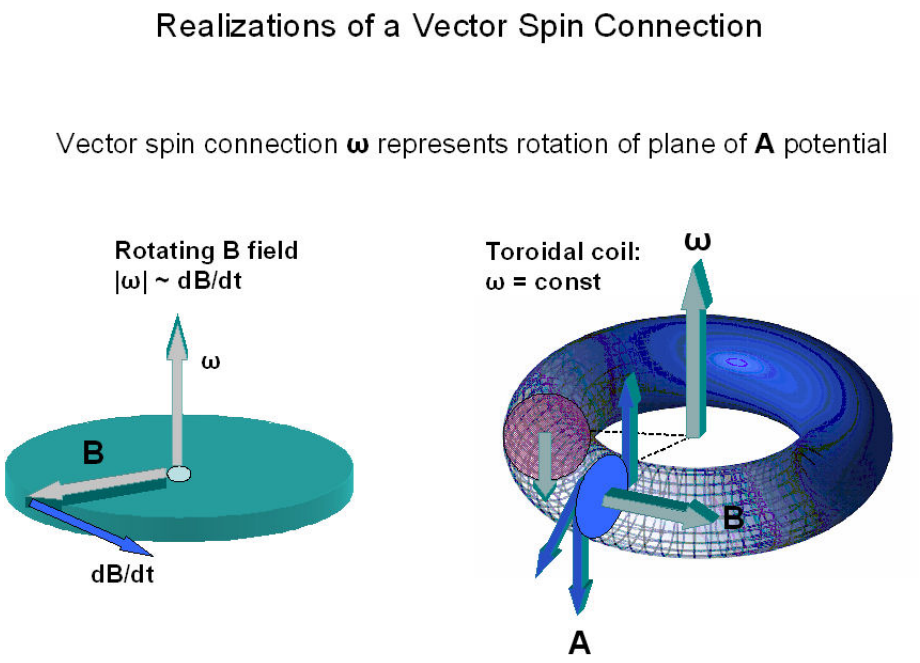

Figure 9: Realizations of a vector spin connection by magnetic fields.

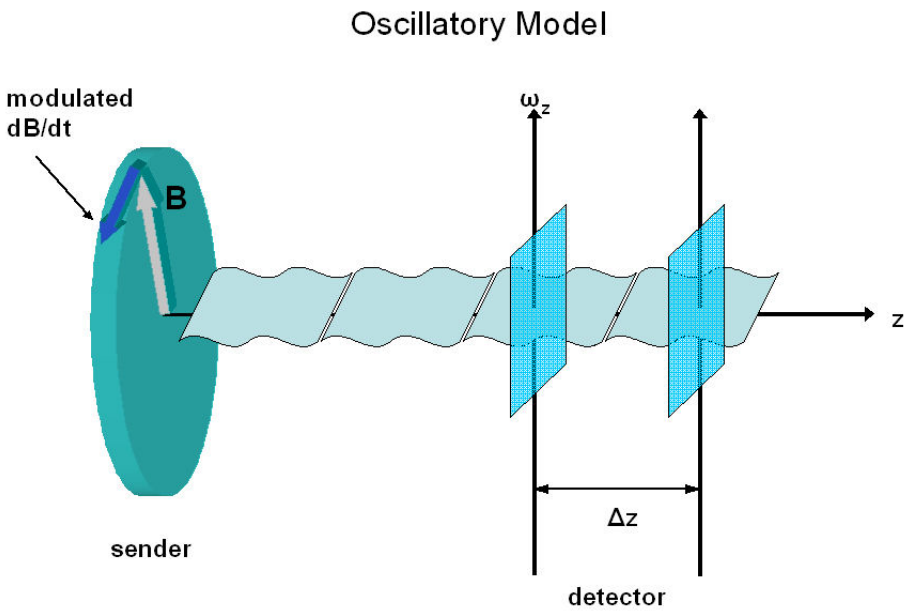

Figure 10: Realization of model 1 (oscillatory model).

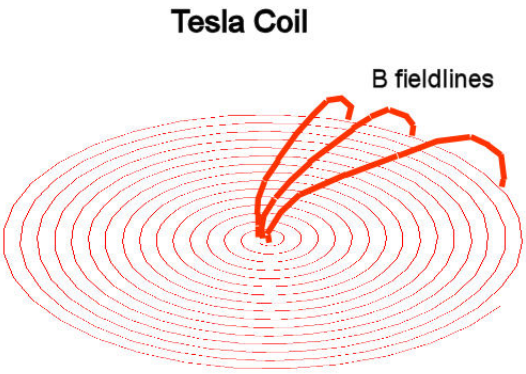

Figure 11: Magnetic field of a Tesla coil.

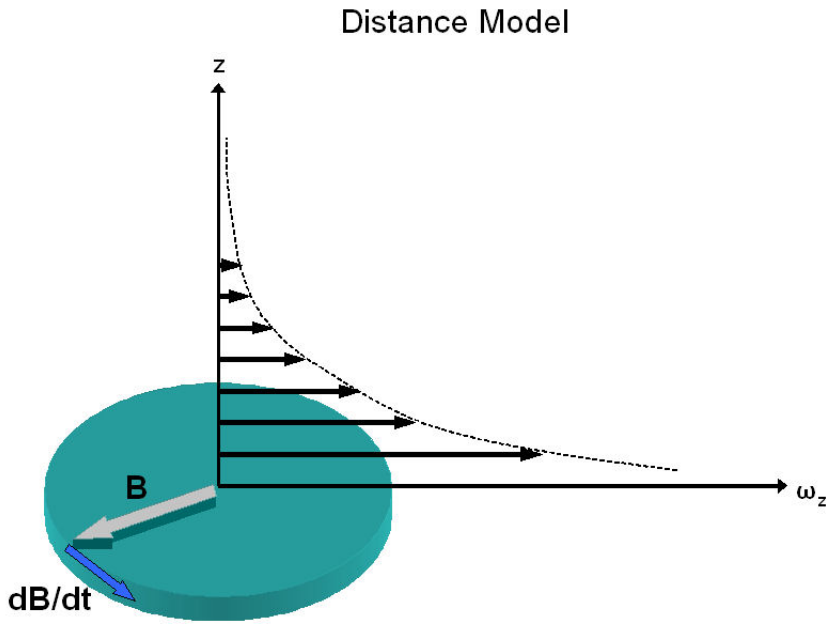

Figure 12: Realization of model 2 (distance model).

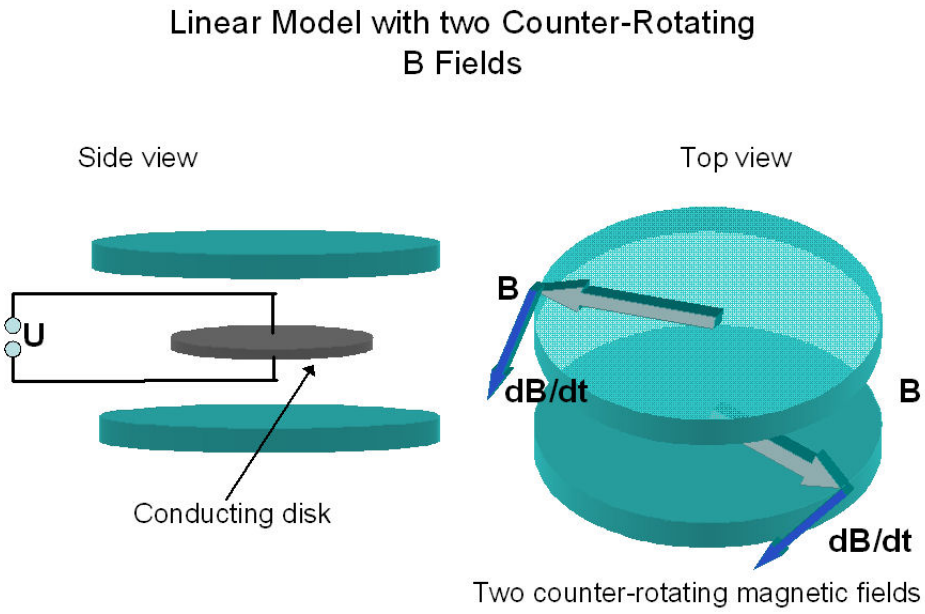

Figure 13: Realization of model 3 (linear model) with two counter-rotating B fields.

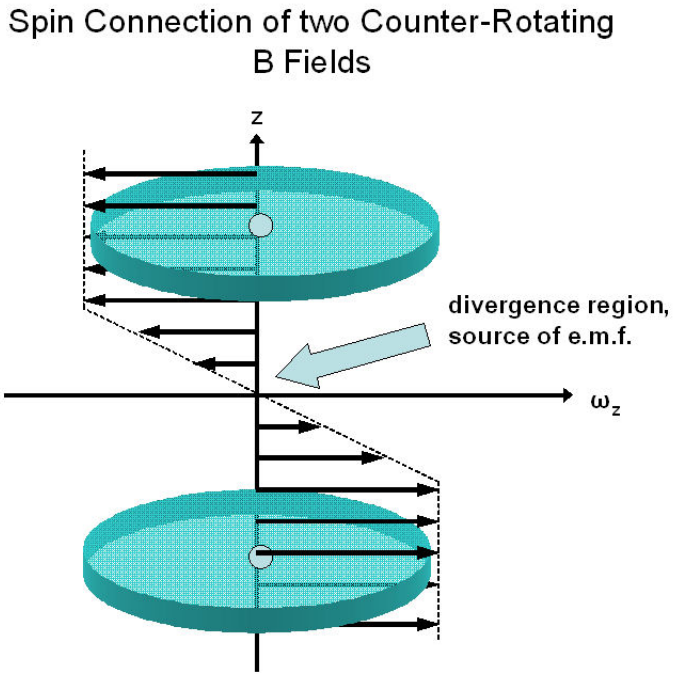

Figure 14: Spin connection of two counter-rotating B fields.

For $\gamma_1 < 0$ the gaussian terms have positive exponents, the solution grows over-exponentially for $z \to \infty$. This is a giant resonance. The driving force does not play a role in this model, but can (in conjunction with the initial conditions) lead to a sign change of the resonance.

3 Propositions for experimental realizations

After it has been shown that the three models are candidates for resonance effects, in this section a technical realization of these models is proposed. This is mainly how to construct a spin connection as used in the models. The vector spin connection $\boldsymbol{\omega}$ can be considered to be a rotation vector of the plane of the vector potential from which the magnetic field is generated. For example a toroidal coil or solenoid exhibits a constant rotation of the A plane per unit angle and therefore creates a constant spin connection, see Fig. 9, right-hand side. A linear coil does not produce a spin connection since the magnetic field vectors are parallel and the A plane does not change.

As an alternative method, the rotation of the A plane can be enforced by a rotating magnetic field, see Fig. 9, left-hand side. The time-frequency of the rotation ω_t can be related to the z component of the spin connection ω_z by

$$\omega_t = c\,\omega_z. \tag{28}$$

This has to be confirmed experimentally but is taken as a working hypothesis here. Then a spin connection can be created by a rotating magnetic field which is used in standard three-phase AC electromotors.

Model 1

An application of model 1 is shown in Fig. 10. The rotation speed of the B field has to be varied periodically. The oscillating spin connection results by the fact that it is proportional to the time derivative of the B vector:

$$\omega_z \propto \left| \frac{\partial \mathbf{B}}{\partial t} \right|. \tag{29}$$

If two conducting plates are positioned in a distance Δz which correcsponds to a quarter of the wavenlength in Figs. 2 or 3, an enhanced electrical signal can be induced. This would correspond to a "space-time enhanced transmitter" as was reported to have been built by Nicola Tesla. To spin this thought a bit further, a Tesla coil is shown if Fig. 11. The magnetic field lines of this device - although nowhere shown in the literature - must have the form as shown in Fig. 11. Obviously this is a static image of the rotating field in Figs. 9/10. This can be seen as a strong hint that Tesla used effects of the spin connection for is unusual experiments, anticipating hundred years of development in theory.

Model 2

A similar distance effect can be obtained by model 2. Here the spin connection decreases inversely proportional to the distance from the generating field (Fig. 12). According to Fig. 5 an enhancement of the electrical potential is possible for $a_1 > 0$. In case $a_1 < 0$ (Fig. 6) no enhancement is obtained. It

is not clear how these sign conditions can be arranged experimentally. In the simplest case they correspond to two sides of the rotational field area where the spin connections point to different directions, seen from the center. Tests with a Tesla coil could be helpful. The above comments concerning the Tesla coil also apply to this model.

Model 3

The most interesting effects can be expected from model 3. This can be realized by two B fields rotating in parallel planes but different directions, see Fig. 13. The development of the spin connection then changes sign in the middle between the planes as graphed in Fig. 14. From Fig. 7 we expect the potential to take the form of a resonant gaussian function for $\gamma_1 > 0$. Therefore a dielectric or conducting disk centered between the planes of rotation should get a high voltage, compared to earth potential. In contrast to model 2, it is quite clear how the case $\gamma_1 < 0$ can be realised. The direction of rotation has to be reversed in both planes. Fig. 8 teaches us that we will get then a high voltage between both sides of the disk, if it is thick enough (see also left-hand side of Fig. 13). According to Fig. 14 the "source of space-time energy" can be located in this case very well: it is the region where $\boldsymbol{\omega}$ changes sign. From Eq. (13) here we have the condition

$$\boldsymbol{\nabla} \cdot \boldsymbol{\omega} \neq 0, \tag{30}$$

in other words, the divergence of the spin connection acts as a source of voltage. The divergence term acts like a charge density of space-time itself. The mechanism is either a forced oscillation or a divergent solution of the generalized Coulomb law of ECE theory. Compared to the verified space-time device of Bedini [9] which has recently been explained by ECE theory [8], the realizations in this article are of much simpler nature. Therefore a quantitative design of these proposed machines appears feasible.

The results of this paper are intellectual property of the author and publically available under the AIAS License as published on *www.aias.us*.

4 Acknowledgments

The AIAS staff, in particular M. W. Evans, is thanked for many interesting discussions.

References

[1] M. W. Evans, "Generally Covariant Unified Field Theory" (Abramis, Suffolk, 2005 onwards), volumes one to four, volume five in prep. (Papers 71 to 93 on www.aias.us).

[2] L. Felker. "The Evans Equations of Unified Field Theory" (Abramis, Suffolk, 2007).

[3] H. Eckardt, L. Felker, "Einstein, Cartan, Evans - Start of a New Age in Physics ?", www.aias.us, 2005.

[4] H. Eckardt, "ECE Engineering Model (Slide set)", www.aias.us, 2008.

[5] H. Eckardt, "How do space energy devices work?", www.aias.us, 2007.

[6] M. W. Evans and H. Eckardt, Paper 61 of www.aias.us, published in volume four of ref. [1].

[7] M. W. Evans and H. Eckardt, Paper 63 of www.aias.us, published in volume four of ref. [1].

[8] M. W. Evans and H. Eckardt, Paper 94 of www.aias.us, to be published in volume six of ref. [1].

[9] J. Bedini, US patents on the Bedini devices: US Patent No. 6,392,370 (2002), 6,545,444 (2003), 20020097013 (2002), 20020130633 (2002); industry certification test report (German TUV, 2002) under http://www.icehouse.net/john34/bedinibearden.html.

[10] J. B. Marion and S. T. Thornton, Classical Dynamics of Particles and Systems (Saunders College Publishing, Fort Worth Philadelphia, fourth Ed., 1995).